Article

Inflammatory Properties of Iron-Containing Carbon Nanoparticles

W. James Waldman, Robert Kristovich, Deborah A. Knight, and Prabir K. Dutta

Chem. Res. Toxicol., **2007**, 20 (8), 1149-1154 • DOI: 10.1021/tx700008n • Publication Date (Web): 3 August 2007

Inflammatory Properties of Iron-Containing Carbon Nanoparticles

W. James Waldman,*,† Robert Kristovich,‡ Deborah A. Knight,† and Prabir K. Dutta*,‡

Department of Pathology, The Ohio State University College of Medicine, 4160 Graves Hall, 333 West 10th Avenue, Columbus, Ohio 43210, and Department of Chemistry, The Ohio State University, 120 West 18th Avenue, Columbus, Ohio 43210

Received January 9, 2007

Inflammatory responses following exposure of carbon nanoparticles to human macrophage and endothelial cells were employed as indicators of particulate biological activity. Hundred nanometer carbon particles (nC) with and without nonextractable surface-bound iron were synthesized using a templating approach, and human monocyte-derived macrophages (MDM) were exposed to various concentrations of these particulates. Supernatants recovered from MDM 24 h postexposure were assayed for the inflammatory cytokine tumor necrosis factor-α (TNFα) by a quantitative ELISA and tested for their ability to induce expression of intercellular adhesion molecule-1 (ICAM-1) on human endothelial cells (EC) by immunofluorescence flow cytometry. Data generated by these experiments demonstrated that nC-Fe was far more biologically active than nC. In addition, the chemical reactivity of nC-Fe toward decomposition of hydrogen peroxide to form hydroxyl radicals was significantly higher than that of nC and correlated well with the increase in the strength of the inflammatory response, though a direct proof of creation of hydroxyl radicals in the biological system is not provided. Comparison with micrometer-sized carbon and carbon–iron particles suggests that the chemical and biological reactivity is correlated with surface area.

Introduction

Epidemiological studies have demonstrated an association between levels of airborne particulate matter with a mass median aerodynamic diameter of ≤ 2.5 μm ($PM_{2.5}$) and morbidity and mortality. Specific particulate-associated disease entities implicated by these studies include chronic bronchitis and interstitial fibrosis, exacerbation of asthmatic episodes, and respiratory infectious diseases, as well as cardiovascular complications such as ischemic heart disease and stroke (*1, 2*).

In support of the epidemiological observations cited above, a recent study of lung tissue acquired at autopsy from lifelong residents of Mexico City, a region of sustained high levels of airborne particulates, demonstrated extensive particulate deposition and greatly thickened, fibrotic airway walls as compared to lung tissue of individuals from Vancouver, BC, a region of low ambient particulate levels (*3*). In vitro studies and animal experiments have documented a number of biological and pathological responses to particulate exposure, including enhancement of cytokine, chemokine, and intracellular oxidant production by macrophages and airway epithelial cells following phagocytosis of particulates (*4–7*), impairment of chemotactic motility of particulate-laden macrophages (*8*), acute and chronic pulmonary inflammation in vivo following experimental particulate administration or natural exposure in animals and humans (*9–12*), and the subsequent development of alveolar epithelial hyperplasia and progressive pulmonary fibrosis (*9, 12*).

The ultrafine component of $PM_{2.5}$ (particles less than 100 nm in diameter, $PM_{0.1}$) has been suggested to be of major etiologic significance in detrimental health effects (*13*). While ultrafine particles make up only 1–8% of the total mass of particulate air pollution in the atmosphere, because of their smaller size, they are the most abundant component of urban PM_{10}. Urban airborne ultrafine particulates are produced by combustion sources. These particles evolve from the molecular level, allowing the primary particle size to be very small, often in the range of 5–20 nm (*14*). However, they tend to agglomerate in the atmosphere, forming larger particles 100–200 nm in size (*15*). A common example of such particles is diesel emission particulates, with a carbon core. Ambient particulates are variable mixtures of many types of particles; hence, relationships between specific physicochemical properties of particulates and the mechanisms and intensity of biological responses induced following exposure can be more clearly elucidated with simplified model particulates.

Several studies have been reported with ultrafine C particles using animal models, and correlations with inflammatory responses have been discovered (*16–19*). We have previously demonstrated that 1 μm C and iron-containing C (C-Fe) particles have dramatically differing biological responses, even though they are similar in every way except 1.8% of the surface iron on the C-Fe particle (*20*). In the current study, the focus is on $\sim$100 nm carbon particles, into which iron, a component that has been linked to increases in levels of inflammatory cytokines and endothelial activation, was incorporated. Since both the macrophage and the endothelium are major components in the inflammatory response, our studies have focused on these cells. Specifically, we have tested the hypothesis that surface-bound nonextractable iron internalized by human macrophages promotes a macrophage inflammatory response, and that soluble factors elaborated by such macrophages activate endothelial cells to an inflammatory phenotype. Previous studies have shown that extractable iron from respirable particulates can cause biological effects, and this study extends such biological effects to iron firmly held on the particle surface (*21*).

* To whom correspondence should be addressed. E-mail: james.waldman@osumc.edu or dutta.1@osu.edu. Telephone: (614) 292-7772. Fax: (614) 292-5849.

† The Ohio State University College of Medicine.

‡ Department of Chemistry, The Ohio State University.

10.1021/tx700008n CCC: $37.00
Published on Web 08/03/2007

Experimental Methods

Particle Synthesis. Zeolite Y crystallites ~100 nm in size were synthesized according to previously published procedures (*22*), and commercial micrometer-sized zeolite Y was obtained from Union Carbide (LZY-52). The synthesis of carbon particle replicas proceeds through an acid-catalyzed condensation reaction of phenol and paraformaldehyde monomers using zeolite Y as a template for the reaction (*20, 23*). Prior to use, all zeolites were sodium exchanged and calcined in oxygen for 12 h. Acid groups were introduced into the zeolite by ion exchange with NH_4Cl, followed by decomposition of the ammonium ions under vacuum at 500 °C. The zeolite was cooled to room temperature, and solid phenol (0.21 g of phenol/g of zeolite) was added. A weak vacuum was pulled on the system, and the temperature was increased slowly to 60 °C. Solid paraformaldehyde (0.25 g of paraformaldehyde/g of zeolite) was added to the zeolite/phenol material, and the temperature was increased very slowly to 120 °C in a nitrogen environment. At this point, the solid material turned red as the phenol–paraformaldehyde-cross-linked polymer formed. The solid material was held at 120 °C for 5 h to allow for complete polymerization. For synthesis of iron-containing particulates, 5 wt % iron was added by spiking the samples with a 0.05 M ferrous acetate solution. The zeolite/polymer mix was pyrolyzed at 800 °C for 19 h under flowing argon. The zeolite template was removed by etching in 48% hydrofluoric acid for 6 h. Repeated washings with copious amounts of water are required to thoroughly remove HF prior to use (total water volume used exceeded 500 mL). Ultrafine particles required ultracentrifugation, at 25 000 rpm, between washings and for collection.

Particle Characterization. The surface chemical composition of particulates was determined by X-ray photoelectron spectroscopy using a Kratos Ultra Axis XPS instrument with an aluminum source. Particle morphology was measured using a Tecnai TF-20 transmission electron microscope.

Endothelial Cells and Macrophages. Human umbilical vein endothelial cells (HUVEC) and human pulmonary microvascular EC (HPMVEC) were obtained and propagated as previously described (*20, 24*). Peripheral blood mononuclear cells (PBMC) were isolated from buffy coats (purchased from the American Red Cross) by density gradient sedimentation through Ficoll-Hypaque (Histopaque, Sigma Chemical Co., St. Louis, MO) (*25*). PBMC were suspended in RPMI 1640 (Gibco), supplemented with 10% pooled normal human serum. To promote differentiation of monocytes into the macrophage phenotype, PBMC were incubated for 5–7 days in Teflon plates at 37 °C in a humidified atmosphere of 5% CO_2 and 95% air (*26*).

Following incubation, cells were recovered from plates, pelleted by centrifugation, resuspended in fresh culture medium, and transferred to 24-well plastic tissue culture plates (Costar, Corning, Inc., Corning, NY). Following incubation for 18–24 h, supernatants containing nonadherent cells were removed and adherent cells were washed three times with PBS. The adherent monocyte-derived macrophages (MDM) were supplied with fresh culture medium and used within 48 h.

Treatment of Macrophages with Particulates. Particulates were sterilized by steam autoclave and suspended in phosphate-buffered saline (PBS) at a concentration of 5 μg/mL. Particulates were sonicated and immediately added to MDM at a series of nontoxic concentrations (0–25 $\mu g/cm^2$ of surface area). To promote contact and internalization of particulates by MDM, the plates were centrifuged at 1200*g* for 15 min, incubated for 30 min at 37 °C in a humidified atmosphere of 5% CO_2 and 95% air, then supplied with additional medium (0.4 mL/well), for a total supernatant volume of 0.5 mL, and incubated for 24 h. Following incubation, culture supernatants were recovered, clarified by centrifugation (16000*g* for 10 min), and stored at −80 °C until assay.

Transmission Electron Microscopy of MDM. Particulate-treated MDM (and untreated controls) were suspended by gentle scraping following incubation for 15 min in 1% EDTA at 4 °C. Cells were washed twice in PBS, then fixed for 18–24 h in 3% cacodylate-buffered glutaraldehyde, and processed for transmission electron microscopy. Sections were examined on a Zeiss EM 900 microscope (Carl Zeiss SMT Inc., Thornwood, NY) equipped with a Mega View III digital camera (Soft Imaging System, GmbH, Munster, Germany).

Quantitation of TNFα in MDM Culture Supernatants. TNFα elaborated by particulate-treated MDM (or untreated controls) was quantitated by a colorimetric ELISA (Quantikine R&D Systems, Inc., Minneapolis, MN). Absorbance was measured at 450 nm on a BioTek FL600 microplate reader (BioTek Instruments, Inc., Winooski, VT). Mean optical densities (OD) were calculated from absorbance values of duplicate wells, and absolute TNFα concentrations in supernatants were determined by correlation of OD values with those generated by a seven-step titration of known quantities of TNFα.

Assay of Macrophage-Mediated Endothelial Activation. HUVEC or HPMVEC were incubated with supernatants recovered from particulate-treated MDM cultures (or untreated MDM) and then assayed by immunofluorescence flow cytometry for expression of intercellular adhesion molecule-1 (ICAM-1). Additional controls included untreated quiescent EC, EC treated with 300 IU/mL human recombinant tumor necrosis factor-α (TNFα; R&D Systems, Minneapolis, MN) as a positive control for adhesion molecule induction, and EC treated with clarified lysates of sonicated MDM.

To specifically identify the inducing agent produced by particulate-treated MDM, supernatants recovered from MDM cultures were incubated for 1 h with 0.25 μg/mL polyclonal rabbit anti-human tumor necrosis factor-α (TNFα, Genzyme Diagnostics, Cambridge, MA) or with 0.25 μg/mL irrelevant polyclonal rabbit IgG (Jackson Immunoresearch Laboratories, West Grove, PA) prior to addition of supernatants to endothelial monolayers. To rule out the possibility that MDM responses were due to endotoxin contamination of particulates, a subset of the experiments described above were conducted in the presence of 10 μg/mL polymyxin B (Sigma), a concentration shown to completely neutralize the effects of 100 pg/mL lipopolysaccharide (LPS; Sigma).

Measurement of Hydroxyl Radical Production by Particles. Five milligrams of particles was weighed and suspended in 500 μL of a phosphate-buffered saline (pH 7.4) solution. To this suspension was added 100 μL of 5,5-dimethyl-1-pyrolline *N*-oxide (DMPO, 97% pure; Aldrich Chemical Co.), along with 50 μL of a 30% hydrogen peroxide solution (Mallinkrodt AR). The solution was shaken in the dark for 15 min. The particles were removed by centrifugation, and the solution was analyzed by electron paramagnetic resonance (EPR) spectroscopy (Bruker ESP300 ESR spectrometer). EPR was performed with a modulating frequency of 100 kHz with a modulating amplitude of 2.090 G. The microwave power was 6.32 mW. To assure that the observed spectra are indeed from the formation of hydroxyl radicals, a number of blanks, including particles with DMPO without hydrogen peroxide, PBS with DMPO and hydrogen peroxide, and the particles in PBS without DMPO or hydrogen peroxide, were also examined.

Results

Description of Particulates. C particles were synthesized using zeolite as the host for a phenol–paraformaldehyde polymerization reaction. For the synthesis of the nanometer particles, a synthetic ~100 nm zeolite Y was used as the template for the polymerization reaction. The zeolite-polymer was then pyrolyzed at 800 °C, in argon, to graphitize the polymer material. The zeolite template was etched with HF, which dissolves the aluminosilicate, leaving behind a carbon particle (*20*).

The transmission electron micrograph (TEM) shown in Figure 1a confirms that the C particles are ~100 nm in size, and powder X-ray diffraction data show these particles to be amorphous. The material has an octahedral morphology, similar to that of the starting zeolite. Surface elemental analysis reveals a carbon material, with a small contribution from silicon and no

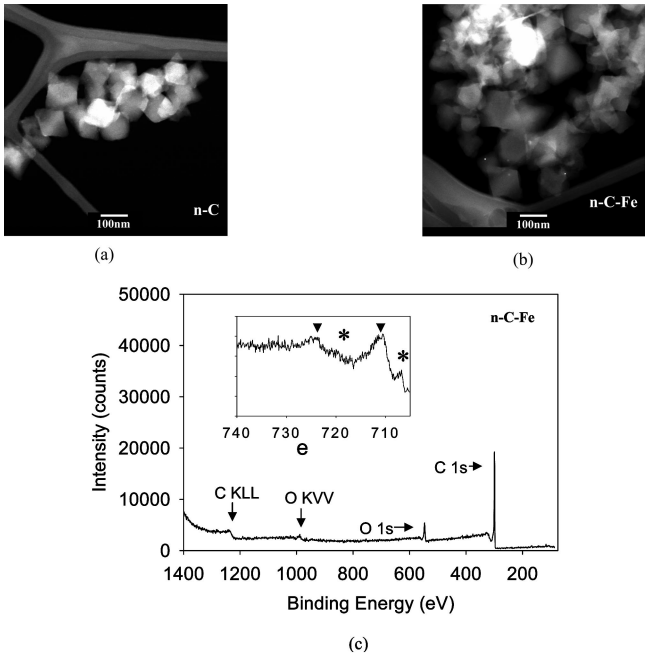

Figure 1. Transmission electron micrographs of (a) nC and (b) nC-Fe. (c) X-ray photoelectron spectroscopy data for nC-Fe. The inset shows the Fe3p binding region: (▼) Fe^{3+} and (*) Fe^{2+}.

aluminum. Nanometer carbon–iron (nC-Fe) particles were synthesized by impregnation with 5 wt % ferrous iron prior to pyrolysis in argon. The TEM in Figure 1b shows that the morphology of the nC-Fe particles is similar to that of the nC particles. XPS shown in Figure 1c indicates that iron was indeed incorporated into the nC-Fe particles, and that some of the ferrous iron was oxidized, resulting in a mixture of Fe^{2+} (29% of the total iron; binding energy for the iron $2p_{3/2}$ peak of 708.0 eV) and Fe^{3+} (71% of the total iron; binding energy for the iron $2p_{3/2}$ peak of 711.7 eV) (Figure 1c, inset). The total surface iron loading was calculated from the XPS to be 3.5% by mass.

Scanning electron microscopy (SEM) of the micrometer-sized C particles shows they are indistinguishable from the starting zeolite particles, as we showed previously (*20*). Surface elemental analysis of μC-Fe also shows a mixture of Fe^{2+} (45% of the total iron; binding energy for the iron $2p_{3/2}$ peak of 708.0 eV) and Fe^{3+} (55% of the total iron; binding energy for the iron $2p_{3/2}$ peak of 711.7 eV). The calculated loading level of surface iron was 6.4% by mass.

Internalization of Particles by Macrophages. While in our previous studies of macrophage activation by 1 μm particulates, internalized particles were easily viewed by phase contrast microscopy (*20, 27*), transmission electron microscopy was required for verification of internalization of nC particulates in the current experiments. Human MDM were differentiated and treated with sonicated particulates as described above, then harvested, fixed, and embedded 24 h later. As demonstrated by transmission electron microscopy, both nC and nC-Fe particles were found to be internalized by the cells and appeared to be localized in phagolysosomes (Figure 2). Similar to our earlier observations of 1 μm particulates (*27*), nC particles appeared to remain well-dispersed within macrophage phagolysosomes (Figure 2b) while nC-Fe tended to form agglomerates of up to several hundred nanometers (Figure 2c). However, phase contrast microscopic observation of cells immediately following addition of particulates to cells, centrifugation, and a 1 h incubation revealed only very fine, barely visible granular material, suggesting that agglomeration occurred during or following internalization by macrophages.

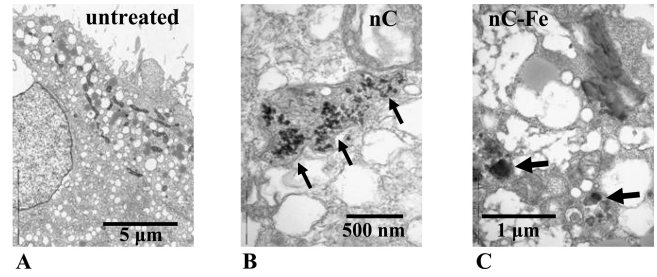

Figure 2. Transmission electron micrographs of (A) untreated macrophages and macrophages treated with (B) nC and (C) nC-Fe.

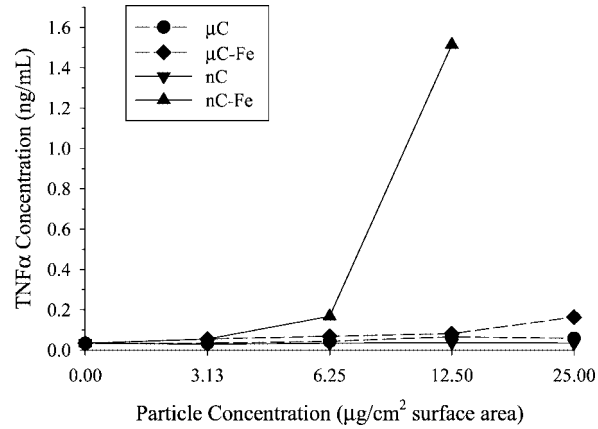

Figure 3. Particulate-mediated induction of TNFα in macrophages. MDM were treated with various concentrations of nC, nC-Fe, μC, and μC-Fe. Culture supernatants were recovered 24 h postexposure, clarified by centrifugation, and assayed for TNFα concentration with an ELISA. Data points represent mean values calculated from duplicate microtiter wells. Data are representative of results of three replicate experiments conducted with MDM isolated from three individual donors. Note that the concentration of TNFα generated by 25 μg of nC-Fe/cm^2 exceeded the upper measurable limit of the assay. Data generated by experiments conducted with MDM isolated from the two remaining donors appear in the Supporting Information.

Particulate-Mediated Induction of TNFα Production by Macrophages. To quantitate particulate-mediated TNFα production by macrophages, supernatants of particulate-treated (or untreated) MDM were analyzed by an ELISA. As shown in Figure 3 (representative of three replicate experiments conducted with MDM isolated from three individual donors), while μC-Fe induced modest production of TNFα by MDM (~0.15–0.2 ng/mL) only at the highest particulate concentration of 25 μg/cm^2, nC-Fe induced a dose-dependent elaboration of TNFα by MDM, reaching a level of >1.5 ng/mL in response to treatment with 12.5 μg/cm^2 (data generated by experiments conducted with MDM isolated from the two remaining donors appear in the Supporting Information). Data points represent mean values determined from duplicate microtiter wells. It should be noted that TNFα production induced by 25 μg/cm^2 nC-Fe exceeded the upper measurable limit of the assay. In contrast, TNFα produced by nC- and μC-treated MDM was below the detection limit of the assay at all particulate concentrations (up to 25 μg/cm^2). To verify that these observations were not the result of selective binding of TNFα to nC or μC, culture medium supplemented with recombinant TNFα (1 ng/mL) was incubated for 1 h at 37 °C with or without carbon particles (100 μg/mL), clarified by centrifugation, and analyzed by a TNFα-specific ELISA. Curves generated by serial dilutions of each sample demonstrated no differences in TNFα concentrations between samples (data not shown).

Macrophage-Mediated Endothelial Activation by Nanoparticulates. As a functional correlate to particulate-

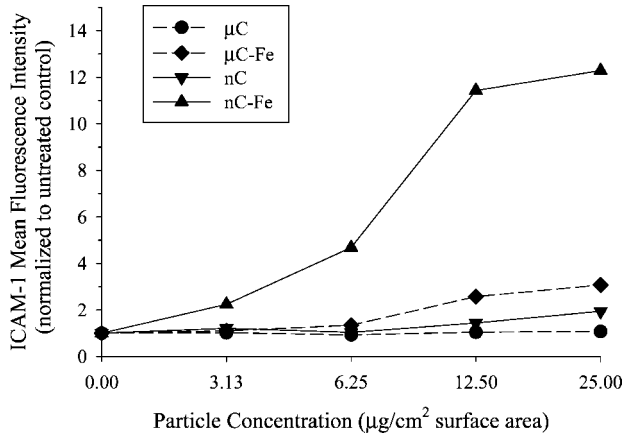

Figure 4. Macrophage-mediated endothelial ICAM-1 induction by particulates. Human umbilical vein endothelial cells (HUVEC) or human pulmonary microvascular EC (HPMVEC) were incubated for 24 h with supernatants recovered from MDM treated with various concentrations of μC, nC, μC-Fe, and nC-Fe. EC were then harvested, stained with a FITC-conjugated antibody specific for ICAM-1, and analyzed by fluorescence flow cytometry (5000 cells/sample). Data are representative of results of three replicate experiments conducted with MDM isolated from three individual donors. Data generated by experiments conducted with MDM isolated from the two remaining donors appear in the Supporting Information.

induced TNFα production by MDM, and to model the impact of soluble factors elaborated by particulate-exposed macrophages upon proximal endothelium, expression of ICAM-1 by HUVEC or HPMVEC incubated with clarified supernatants of particulate-treated (or untreated) MDM was assayed by immunofluorescence flow cytometry.

Data generated by a representative experiment (of three replicates conducted with MDM isolated from three individual donors), expressed as mean fluorescence intensity normalized to untreated controls, are shown in Figure 4 (data generated by experiments conducted with MDM isolated from the two remaining donors appear in the Supporting Information). As we have previously demonstrated, supernatants recovered from macrophages treated with μC had no impact upon endothelial ICAM-1 expression (*20*), and this behavior is reproduced in Figure 4. Similarly, supernatants recovered from nC-treated macrophages induced only a slight increase (~2-fold) in the level of endothelial ICAM-1. While supernatants recovered from macrophages treated with 25 μg of μC-Fe/cm^2 induced an approximately 3-fold enhancement in the level of endothelial ICAM-1, supernatants recovered from macrophages treated with nC-Fe at all concentrations induced higher levels of endothelial ICAM-1 (up to 12-fold over those of untreated controls at 25 μg/cm^2).

These endothelial responses were not due simply to macrophage components released as a consequence of cellular injury since no ICAM-1 enhancement was induced by clarified supernatants of untreated MDM disrupted by sonication (data not shown). In addition, MDM-mediated endothelial activation was not attributable to endotoxin carried into the MDM on the particulates, since particulate treatment in the presence of 10 μg/mL polymyxin B, a concentration shown to completely neutralize the effects of 100 pg/mL LPS, had no impact upon endothelial ICAM-1 induction (data not shown). Finally, the inducing agent elaborated by particulate-treated MDM was identified as TNFα by the complete attenuation of MDM-induced ICAM-1 by addition of a blocking antibody specific for TNFα to supernatants prior to their incubation with EC, as demonstrated by the fluorescence flow cytometry data presented in Figure 5.

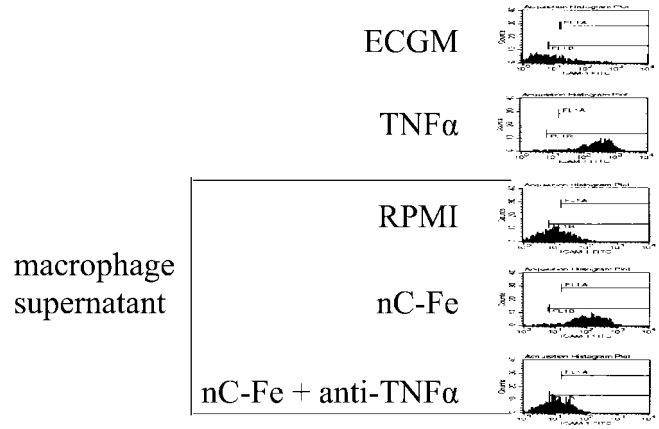

Figure 5. Neutralization of macrophage supernatant-mediated induction of endothelial ICAM-1 by a blocking antibody specific for TNFα. Human umbilical vein endothelial cells (HUVEC) or human pulmonary microvascular EC (HPMVEC) were incubated for 24 h with endothelial cell growth medium (ECGM), ECGM supplemented with 300 IU/mL TNFα, or supernatants recovered from untreated MDM (RPMI), supernatants of nC-Fe-treated MDM (25 μg/cm^2), or supernatants of nC-Fe-treated MDM in the presence of an antibody with specific blocking activity against TNFα. EC were then harvested, stained with a FITC-conjugated antibody specific for ICAM-1, and analyzed by fluorescence flow cytometry (5000 cells/sample). Data are representative of results of two replicate experiments conducted with MDM isolated from two individual donors.

Figure 6. Measure of hydroxyl radical production. DMPO-OH adduct formed in solution as determined by electron paramagnetic resonance spectroscopy after exposure of μC, nC, μC-Fe, and nC-Fe particulates to H_2O_2.

Determination of Fenton Activity of Particles. The ability of the particles to catalyze the decomposition of hydrogen peroxide to hydroxyl radicals through Fenton chemistry was assessed by spin trapping with 5,5-dimethylpyrroline *N*-oxide (DMPO). The four-line first-derivative ESR signal (1:2:2:1 quartet) characteristic of the hydroxyl adduct, 2,2-dimethyl-5-hydroxy-1-pyrrolidinyloxyl (DMPO-OH) with a hyperfine splitting constant of 14.3 G, was clearly observed after exposure of nC-Fe and μC-Fe particles to hydrogen peroxide, with the former giving the stronger signal. No signal was generated by nC and only a weak signal by μC (Figure 6).

Discussion

Epidemiological studies have demonstrated an association between increases in morbidity and mortality and increases in the level of airborne $PM_{2.5}$ (*1, 2*). This increase in morbidity and mortality has been linked to several disease processes, many of which involve inflammation. Inflammation is controlled by a series of intracellular and extracellular signaling processes whose function is to signal the presence of a foreign body or

infectious agent, to clear or contain the agent, and to begin the wound repair process. This study was aimed at examining the role of nonextractable surface iron in the secretion of the cytokine TNF-α by MDM and in the consequent expression of the proinflammatory adhesion molecule ICAM-1 on proximal EC. While we recognize that particulate exposure may induce the expression of a number of additional cytokines, chemokines, and receptors (*4–7*), the study presented here was not intended to document an array of responses. Rather, we have focused upon the induction of TNFα, a major mediator of endothelial recruitment and extravasation of inflammatory cells, as an indicator of the potential proinflammatory impact of surface-bound iron.

Human monocyte-derived macrophages were utilized in this study because of the critical role of the macrophage in phagocytizing particles in the lung and the role that the macrophage plays in mediating inflammation. Activated macrophages, through exposure to a microorganism or toxin, secrete cytokines that signal the need for recruitment of inflammatory cells to the site of an injury or infection. Human endothelial cells were also utilized because of the pro-inflammatory role they play in recruiting circulating leukocytes through their ability to inducibly express endothelial leukocyte adhesion molecules.

Macrophages exposed to high concentrations (200 μg/mL) of ultrafine carbon black (14 nm) have been shown to produce a modest level of TNF-α, which can be blocked by introduction of the calcium channel blocker verapimil (*28*). It has been proposed that production of reactive oxygen species (ROS) leads to the oxidation of calcium pumps in the endoplasmic reticulum (*28*). The role of free radicals and reactive oxygen species created upon ultrafine particle inhalation in causing inflammation is being recognized for different types of particulates (*29*).

Iron can lead to the formation of hydroxyl radicals through the Fenton mechanism. Iron-containing particles have been proposed as a mechanism of introducing unregulated iron into cells (*20, 21, 30*). Soluble iron has been shown to induce the expression of TNF-α in Kupffer cells, which was preceded by an increase in the level of hydroxyl radicals (*31*).

Particles used in this study have surface-bound nonextractable iron, which is redox active, which is evident from the Fenton chemistry. In a previous study, we have reported biological assays with micrometer-sized C (μC) particulates, but the published results from the micrometer-sized particles cannot be directly compared since the iron incorporation methods were different (*20*). In the previous study, the iron was incorporated by ion exchanging iron into the zeolite prior to polymerization of the phenol–paraformaldehye polymer in the pores of the zeolite (*20*), whereas in this study, the iron was impregnated into the sample after formation of the phenol–paraformaldehyde polymer. Therefore, we prepared μC-Fe using the impregnation method which resulted in μC-Fe, with 6.4% iron by mass, as compared to ∼100 nm nC-Fe with 3.5% iron by mass.

The nC-Fe particles produced 10 times more hydroxyl radicals than the μC-Fe, based on the area under the main peak of the DMPO-OH four-line spectra (Figure 6). At a loading level of 12.5 μg of particles/cm^2, the MDM exposed to nC-Fe produce 1.5 ng of TNFα/mL, and at 25 μg of particles/cm^2, the μC-Fe particle exposed MDM produces 0.18 ng of TNFα/mL (data not shown). A functional assay of expression of ICAM-1 by EC exposed to supernatants recovered from nC-Fe- and μC-Fe-treated MDM showed a 6-fold increase in the level of ICAM-1 (25 μg of particles/cm^2). Assuming spherical particle shapes, the ∼100 nm particle used in this study has 10 times the surface area of the 1 μm particles but a level of surface iron that is 1.8 times lower. So, just on the basis of surface area arguments, the biological effect between the two particles sizes should differ by a factor of 6, and this number is consistent with the results from the Fenton chemistry (factor of 10), the macrophage TNFα production (a factor of >9), and the endothelial ICAM-1 expression (factor of 6). We are currently examining if such a semiquantitative correlation holds as particle sizes become even smaller, thereby providing a surface area-based model for estimating the biological activity.

Conclusions

In summary, the data presented here support the hypothesis that particle size and surface chemistry have a significant impact upon the biological system. Monocyte-derived macrophages (MDM) exposed to ∼100 nm nC-Fe at a concentration of 12.5 μg of particles/cm^2 produced >1.5 ng of TNFα/mL of culture supernatant. Endothelial cells (EC) exposed to supernatants recovered from MDM treated with 25 μg of nC-Fe/cm^2 expressed 6 times more surface intercellular adhesion molecules (ICAM-1) than EC exposed to supernatants recovered from MDM treated with an equivalent mass of μC-Fe. These observations in the biological system are correlated with the production of hydroxyl radicals from H_2O_2 catalyzed by the iron on the particle surfaces, as measured by electron paramagnetic resonance spectroscopy. However, the formation of reactive oxygen species within the biological system was not studied. This study demonstrates that redox-active nonextractable iron on a particle surface can promote the formation of inflammation markers. On the basis of quantitative comparisons between the chemical and biological effects of nano- and micrometer-sized particles, correlations between surface area and function are apparent.

Acknowledgment. This work was supported in part by NIOSH Grant R01 OH009141 (P.K.D. and W.J.W.).

Supporting Information Available: Data generated by TNFα ELISA and ICAM-1 fluorescence flow cytometry conducted with macrophages isolated from two additional volunteer donors. This material is available free of charge via the Internet at http://pubs.acs.org.

References

(1) Koenig, J. Q., Larson, T. V., Hanley, Q. S., Rebolledo, V., Dumler, K., Checkoway, H., Wang, S. Z., Lin, D. Y., and Pierson, W. E. (1993) Pulmonary-Function Changes in Children Associated with Fine Particulate Matter. *Environ. Res. 63*, 26–38.

(2) Pope, C. A., III, Burnett, R. T., Thun, M. J., Calle, E. E., Krewski, D., Ito, K., and Thurston, G. D. (2002) Lung cancer, cardiopulmonary mortality, and long-term exposure to fine particulate air pollution. *J. Am. Med. Assoc. 287*, 1132–1141.

(3) Churg, A., Brauer, M., Avila-Casado, M. C., and Fortoul, T. I. (2003) Chronic exposure to high levels of particulate air pollution and small airway remodeling. *Environ. Health Perspect. 111* (5), 714–718.

(4) Finkelstein, J. N., Johnston, C., Barrett, T., and Oberdörster, G. (1997) Particulate-cell interactions and pulmonary cytokine expression. *Environ. Health Perspect. 105*, 1179–1182.

(5) Goldsmith, C. A., Imrich, A., Danaee, H., Ning, Y. Y., and Kobzik, L. (1998) Analysis of air pollution particulate-mediated oxidant stress in alveolar macrophages. *J. Toxicol. Environ. Health, Part A 54*, 529–545.

(6) Terada, N., Hamano, N., Maesako, K. I., Hiruma, K., Hohki, G., Suzuki, K., Ishikawa, K., and Konoo, A. (1999) Diesel exhaust particulates upregulate histamine receptor mRNA and increase histamine-induced IL-8 and GM-CSF production in nasal epithelial cells and endothelial cells. *Clin. Exp. Allergy 29*, 52–59.

(7) Barrett, E. G., Johnston, C., Oberdörster, G., and Finkelstein, J. N. (1999) Silica-induced chemokine expression in alveolar type II cells is mediated by TNF-α-induced oxidant stress. *Am. J. Physiol. 276*, L979–L988.

(8) Donaldson, K., Brown, G. M., Brown, D. M., Slight, J., Robertson, M. D., and Davis, J. M. G. (1990) Impaired Chemotactic Responses of Bronchoalveolar Leukocytes in Experimental Pneumoconiosis. *J. Pathol. 160*, 63–69.

(9) Callis, A. H., Sohnle, P. G., Mandel, G. S., Wiessner, J., and Mandel, N. S. (1985) Kinetics of Inflammatory and Fibrotic Pulmonary Changes in a Murine Model of Silicosis. *J. Lab. Clin. Med. 105*, 547–553.

(10) Clarke, R. W., Catalano, P. J., Koutrakis, P., Murthy, G. G., Sioutas, C., Paulauskis, J., Coull, B., Ferguson, S., and Godleski, J. (1999) Urban air particulate inhalation alters pulmonaryfunction and induces pulmonary inflammation in a rodent model of chronic bronchitis. *J. Inhalation Toxicol. 11* (8), 637–656.

(11) Nightingale, J. A., Maggs, R., Cullinan, P., Donnelly, L. E., Rogers, D. F., Kinnersley, R., Chung, K., Barnes, P. J., Ashmore, M., and Newman-Taylor, A. (2000) Airway inflammation after controlled exposure to diesel exhaust particulates. *Am. J. Respir. Crit. Care Med. 162*, 161–166.

(12) Calderón-Garcidueñas, L., Mora-Tiscareño, A., Fordham, L. A., Chung, C. J., García, R., Osnaya, N., Hernández, J., Acuña, H., Gambling, T. M., Villarreal-Calderón, A., Carson, J., Koren, H. S., and Devlin, R. B. (2001) Canines as sentinel species for assessing chronic exposures to air pollutants: Part 1. Respiratory pathology. *Toxicol. Sci. 61* (2), 342–355.

(13) Donaldson, K., Stone, V., Clouter, A., Renwick, L., and MacNee, W. (2001) Ultrafine particles. *Occup. Environ. Med. 58*, 211–215.

(14) Vaglieco, B. M., Merola, S. S., D'Anna, A., and D'Alessio, A. (2002) Spectroscopic analysis and modeling of particulate formation in a diesel engine. *J. Quant. Spectrosc. Radiat. Transfer 73*, 443–450.

(15) Kittleson, D. (1998) Engines And Nanoparticles: A Review. *J. Aerosol Sci. 29* (5/6), 575–588.

(16) Haar, C., Hassing, I., Bol, M., Bleumink, R., and Raymond, P. (2005) Ultrafine Carbon Black Particles Cause Early Airway Inflammation and Have Adjuvant Activity in a Mouse Allergic Airway Disease Model. *Toxicol. Sci. 87* (2), 409–418.

(17) Gilmour, P. S., Ziesenis, A., Morrison, E. R., Vickers, M. A., Drost, E. M., Ford, I., Karg, E., Mossa, C., Schroeppel, A., Ferron, G. A., Heyder, J., Greaves, M., MacNee, W., and Donaldson, K. (2004) Pulmonary and systemic effects of short-term inhalation exposure to ultrafine carbon black particles. *Toxicol. Appl. Pharmacol. 195* (1), 35–44.

(18) Elder, A., Gelein, R., Finkelstein, J. N., Driscoll, K. E., Harkema, J., and Oberdörster, G. (2004) Resveratrol-Associated Renal Toxicity. *Toxicol. Sci. 88* (2), 614–629.

(19) Andre, E., Stoeger, T., Takenaka, S., Bahnweg, M., Ritter, B., Karg, E., Lentner, B., Reinhard, C., Schulz, H., and Wjst, M. (2006) Inhalation of ultrafine carbon particles triggers biphasic pro-inflammatory response in the mouse lung. *Eur. Respir. J. 28* (2), 275–285.

(20) Kristovich, R., Knight, D. A., Long, J. F., Williams, M. V., Dutta, P. K., and Waldman, W. J. (2004) Macrophage-Mediated Endothelial Inflammatory Responses to Airborne Particulates: Impact of Particulate Physicochemical Properties. *Chem. Res. Toxicol. 17* (10), 1303–1312.

(21) Balds, A., and Aust, A. E. (2005) Role of Iron in Inactivation of Epidermal Growth Factor Receptor after Asbestos Treatment of Human Lung and Pleural Target Cells. *Am. J. Respir. Cell Mol. Biol. 32* (5), 436–442.

(22) Schoeman, B. J., Sterte, J., and Otterstedt, J. E. (1994) Colloidal Zeolite Suspensions. *Zeolites 14*, 110.

(23) Johnson, S. A., Brigham, E. S., Ollivier, P. J., and Mallouk, T. E. (1997) Effect of micropore topology on the structure and properties of zeolite polymer replicas. *Chem. Mater. 9* (11), 2448–2458.

(24) Sedmak, D. D., Roberts, W. H., Stephens, R. E., Buesching, W. J., Morgan, L. A., Davis, D. H., and Waldman, W. J. (1990) Inability of Cytomegalovirus-Infection of Cultured Endothelial Cells To Induce HLA Class II Antigen Expression. *Transplantation 49*, 458–462.

(25) Waldman, W. J., Adams, P. W., Orosz, C. G., and Sedmak, D. D. (1992) Lymphocyte-T Activation by Cytomegalovirus-Infected, Allogeneic Cultured Human Endothelial Cells. *Transplantation 54*, 887–896.

(26) Andreesen, R., Picht, J., and Lohr, G. W. (1983) Primary Cultures of Human Blood-Borne Macrophages Grown on Hydrophobic Teflon Membranes. *J. Immunol. Methods 56*, 295–304.

(27) Long, J. F., Waldman, W. J., Kristovich, R., Williams, M., Knight, D., and Dutta, P. K. (2005) Comparison of ultrastructural cytotoxic effects of carbon and carbon/iron particulates on human monocyte-derived macrophages. *Environ. Health Perspect. 113*, 170–174.

(28) Brown, D. M., Donaldson, K., Borm, P. J., Schins, R. P., Dehnhardt, M., Gilmour, P., Jimenez, L. A., and Stone, V. (2004) Calcium and ROS-mediated activation of transcription factors and TNF-α cytokine gene expression in macrophages exposed to ultrafine particles. *Am. J. Physiol. 286*, L344–L353.

(29) Dick, C. A., Brown, D. M., Donaldson, K., and Stone, V. (2003) The role of free radicals in the toxic and inflammatory effects of four different ultrafine particle types. *Inhalation Toxicol. 15* (1), 39–52.

(30) Fach, E., Waldman, J. W., Williams, M., Long, J., Meister, R. K., and Dutta, P. K. (2002) Analysis of the Biological and Chemical Reactivity of Zeolite-Based Aluminosilicate Fibers and Particulates. *Environ. Health Perspect. 110*, 1087–1096.

(31) She, H., Xiong, S., Lin, M., Zandi, E., Giulivi, C., and Tsukamoto, H. (2002) Iron activates NF-κB in Kupffer cells. *Am. J. Physiol. 283* (3), G719–G726.

TX700008N